



Measurement report: Nitrogen isotope ($\delta^{15}\text{N}$) signatures of ammonia emissions from livestock farming: implications for source apportionment of haze pollution

Jinhan Wang¹, Zhaojun Nie¹, Yupeng Zhang¹, Xiaolei Jie^{1,2}, Haiyang Liu¹, Peng Zhao^{1,2,3}, and Hongen Liu^{1,2,3}

¹College of Resources and Environment, Henan Agricultural University, Zhengzhou, Henan 450046, China

²Key Laboratory of Farmland Quality Conservation in the Huang-Huai-Hai Plain, Ministry of Agriculture and Rural Affairs, Zhengzhou 450046, China

³Key Laboratory of Soil Pollution Prevention, Control and Remediation in Henan Province, Zhengzhou 450046, China

Correspondence: Yupeng Zhang (zhangyp@henau.edu.cn) and Hongen Liu (liuhongen7178@126.com)

Received: 11 September 2025 – Discussion started: 18 November 2025

Revised: 27 January 2026 – Accepted: 23 February 2026 – Published: 14 April 2026

Abstract. Ammonia emissions from agriculture are the primary source of atmospheric reactive nitrogen, significantly impacting air pollution, soil acidification, eutrophication of water bodies, and human health. Accurate quantification of ammonia from different sources is crucial for effective mitigation. In this study, the air extraction method was employed to collect gases from livestock farms, and the $\delta^{15}\text{N}$ values of volatilized ammonia (NH_3) from the animal husbandry industry in the southern Huang – Huai – Hai Plain of China were analyzed using stable nitrogen isotopes. The results show that isotopic signatures differ significantly among livestock types: dairy cows ($-20.6\text{‰} \pm 0.8\text{‰}$), laying hens ($-27.4\text{‰} \pm 1.0\text{‰}$), and pigs ($-38.4\text{‰} \pm 1.7\text{‰}$). These livestock-derived signatures are distinct from those associated with combustion sources ($-7.0\text{‰} \pm 2.1\text{‰}$) and traffic emissions ($6.6\text{‰} \pm 2.1\text{‰}$), and they exhibit considerably lower variability than fertilizer-derived signatures. Overall, this work provides high-precision isotopic source signatures for livestock operations, offering essential parameters for regional atmospheric ammonia source apportionment and highlighting the need for locally tailored mitigation strategies.

1 Introduction

Ammonia (NH_3) is a highly reactive and abundant nitrogenous gas in the atmosphere. It is classified as a major alkaline species and readily reacts with sulfuric acid and nitric acid to produce ammonium sulfate ($(\text{NH}_4)_2\text{SO}_4$) and ammonium nitrate (NH_4NO_3) (Kawashima et al., 2023; Kirkby et al., 2011). These compounds can form particulate ammonium salts or interact with organic aerosols to generate secondary aerosols. In moderately polluted environments, the mass fraction of these ammonium-containing particles within $\text{PM}_{2.5}$ is relatively low (Huang et al., 2014; Yang et

al., 2011). Under severe pollution conditions, however, ammonium sulfate, ammonium nitrate, and other ammonium salts can account for up to approximately 50 % of the total $\text{PM}_{2.5}$ mass (Battye, 2003; Beusen et al., 2008; Goebes et al., 2003). As a key precursor of secondary inorganic aerosols, NH_3 is a primary contributor to haze formation and constitutes a substantial component of $\text{PM}_{2.5}$ in polluted atmospheres (Wu et al., 2024; Xiang et al., 2022). Excessive ammonia emissions also drive a range of environmental problems, including soil acidification, climate perturbation, reduced atmospheric visibility, and eutrophication of aquatic

ecosystems (Huang et al., 2012; Jiang et al., 2021). Consequently, reducing NH_3 emissions has recently been proposed as a strategy to mitigate smog pollution in China (Liu et al., 2019).

Over the past few decades, substantial changes in air quality have been observed across many countries worldwide (Boyle, 2017; Warner et al., 2017). Notably, China has consistently ranked first in global ammonia (NH_3) emissions (Liu et al., 2013). Current NH_3 emission inventories identify the principal sources as agricultural activities-including fertilizer application and livestock and poultry farming-and non-agricultural sources, such as combustion processes and vehicular emissions (Bouwman et al., 1997; Schlesinger and Hartley, 1992; Streets et al., 2003). It is widely recognized that agriculture represents the predominant source of atmospheric NH_3 , contributing over 70 % of total emissions (Meng et al., 2017; Xu et al., 2024), accounting for more than 70 % of the total (Ma et al., 2021; Ti et al., 2019), with livestock and poultry farming alone accounting for 50 % to 60 % of agricultural NH_3 emission (Huang et al., 2012; Wang et al., 2018). Despite this, substantial uncertainty remains regarding the contribution of livestock-derived NH_3 to nitrogen deposition (Elliott et al., 2019), and estimating these contributions using satellite remote sensing and livestock emission inventories remains challenging (Beusen et al., 2008; Li et al., 2023a; Van Damme et al., 2018). These conventional approaches typically rely on fixed emission factors, such as unit animal excretion coefficients, which are limited by temporal lags and insufficient spatial resolution, thereby hindering the capture of real-time variations in NH_3 emissions and the resulting nitrogen deposition at the farm scale. In contrast, nitrogen stable isotope analysis ($\delta^{15}\text{N}$) provides a direct and highly effective approach for tracing the sources of NH_3 and NH_4^+ (Bhattarai et al., 2020; Xiao et al., 2020). This methodology relies on the principle that distinct emission sources and environmental processes generally exhibit unique isotopic fingerprints (Elliott et al., 2019; Li et al., 2024; Sui et al., 2020), defined by the ratio of heavy (^{15}N) to light (^{14}N) nitrogen isotopes in collected samples (Song et al., 2021).

Numerous studies have employed stable nitrogen isotope ($\delta^{15}\text{N}$) techniques to quantify the contributions of combustion, transportation, and agricultural activities to atmospheric NH_3 and NH_4^+ (Xiang et al., 2022; Xie et al., 2008). For example, during the corn growing season in Northeast China, $\delta^{15}\text{N}$ values of NH_3 volatilized from farmland exhibited a wide range, from -38.0% to -0.2% . Notably, $\delta^{15}\text{N}$ emission rates were considerably lower during the early stages of corn growth compared to later stages, indicating clear seasonal variation (Song et al., 2024). Under different fertilization regimes, significant differences in $\delta^{15}\text{N}\text{-NH}_3$ emissions were observed, with values fluctuating between -46.0% and -4.7% throughout the volatilization period (Ti et al., 2021). Previous studies report that $\delta^{15}\text{N}\text{-NH}_3$ and $\delta^{15}\text{N}\text{-NH}_4^+$ emissions from combustion sources (-7.6% to $+16.2\%$) predominate in winter, contributing up to 51.6 % of total ammo-

nia emissions (Xiao et al., 2022, 2025; Zhou et al., 2021). In contrast, NH_3 emissions from vehicle exhaust exhibit relatively high $\delta^{15}\text{N}$ values ($13.7 \pm 3.7\%$) (Savard et al., 2017; Xi et al., 2023). However, these emissions are primarily localized in urban environments.

Currently, limited studies have reported the $\delta^{15}\text{N}$ characteristics of ammonia from livestock and poultry farming. Existing data mostly rely on passive sampling methods (Berner and David Felix, 2020; Chang et al., 2016; Ti et al., 2018), which assess $\delta^{15}\text{N}$ changes by collecting wet deposition samples surrounding farms (pig farms: -35.1% to -10.5% ; cattle farms: -24.7% to -11.3%). Additional research has quantified $\delta^{15}\text{N}$ variability in livestock and poultry (-31.0% to -15.0%) through simulated ammonia emissions during manure management processes (Hristov et al., 2009). It is noteworthy that $\delta^{15}\text{N}\text{-NH}_3$ fluctuations in livestock and poultry operations may also depend on animal growth stages and reproductive status

The Bayesian stable isotope mixing model MixSAIR is primarily used to allocate contributions of atmospheric emission sources through isotope analysis. MixSAIR is a stable isotope mixing model based on the Bayesian statistical framework, designed to quantitatively analyze the relative contributions of multiple potential sources to the isotopic composition of observed mixtures. Its fundamental assumption posits that the isotopic signature of a mixture can be expressed as a linear combination of the isotopic characteristics of each source weighted by their proportional contributions, while explicitly accounting for source variability, measurement errors, and isotopic fractionation. (Chang et al., 2016; Walters et al., 2022). However, there is no universally fixed $\delta^{15}\text{N}\text{-NH}_4^+$ value for each emission source. As a result, substantial variations in reported $\delta^{15}\text{N}\text{-NH}_4^+$ values for the same source have been documented across different studies. To date, no research has validated changes in $\delta^{15}\text{N}\text{-NH}_4^+$ resulting specifically from livestock and poultry farm emissions, nor has the relationship between $\delta^{15}\text{N}\text{-NH}_4^+$ from different sources and regional variations been examined. To obtain more accurate assessments of $\delta^{15}\text{N}\text{-NH}_3$ variations associated with ammonia emissions from livestock and poultry farming, and to achieve reliable atmospheric NH_3 source apportionment, it is essential to characterize the correlation between $\delta^{15}\text{N}\text{-NH}_4^+$ from different sources and regional differences. In this study, active dynamic sampling methods were used to collect ammonia emissions from intensive pig farms, dairy farms, and laying hen farms located in the southern region of the Huang-Huai-Hai Plain. Meta-analysis techniques were employed to analyze the $\delta^{15}\text{N}$ signatures of different ammonia emission sources. The specific objectives of this research are: (1) to determine the $\delta^{15}\text{N}\text{-NH}_4^+$ values of emissions from livestock and poultry housing at various growth stages; and (2) to investigate the relationship between $\delta^{15}\text{N}\text{-NH}_4^+$ from different sources and regional variations.

2 Materials and methods

2.1 Sampling points in the study area and sample collection and processing

The sampling experiment at the farm was conducted from 9 May to 6 December 2024. No samples were collected in July and August due to the absence of livestock or poultry during these months. The collected samples covered the entire breeding period of fattening pigs and the period from chicks to peak egg production in laying hens. Throughout the trial period, six batches of samples were obtained, amounting to a total of 120 samples for measuring ammonia emissions from livestock and poultry housing. On days when samples were collected during hazy weather, the air pollution level was classified as severe, whereas samples collected under clean atmospheric conditions corresponded to air quality classified as excellent. The sampling principle is based on active air sampling combined with aqueous absorption. Ambient air was continuously drawn through an impinger containing deionized water, in which gaseous NH_3 was absorbed and converted to dissolved NH_4^+ . After sampling, the absorption solution was quantitatively recovered for subsequent laboratory analysis. Under the applied sampling flow rate and duration, the method detection limit for atmospheric NH_3 was on the order of 3 ppb, which is adequate for resolving ambient concentration variations during the observation period. Potential interferences include the co-collection of particulate NH_4^+ and the absorption of other water-soluble alkaline gases. These effects were minimized by controlled sampling duration, appropriate flow rates, and blank correction procedures, and are considered to have a negligible influence on the measured NH_3 concentrations. Samples were collected using atmospheric samplers (Beijing Ke'an Labor Protection Company) at a flow rate of 0.1 to 2 L min^{-1} , with each sample collected over a duration of 60 min (Ferm, 1979; Harrison and Kitto, 1990; Heaton, 1986). All NH_3 samples were collected at a constant and identical flow rate throughout the study period, with all flow rates complying with the National Standard GB 3095-2012.

The intensive fattening pig farm is located in Luoyang City, Henan Province (112.71°E , 34.52°N), with no other livestock operations in the surrounding area. The sampled fattening pig farm houses 2600 pigs distributed across four fully enclosed pig houses. One of these houses was selected as the target sampling site. The sampling procedure was as follows: an atmospheric sampler was positioned 2.0 m from the exhaust vent of the livestock and poultry house at a height of 1.6 m, corresponding to the central height of the exhaust outlet. The sampling duration was set to 60 min, with the gas flow rate maintained at 2 L min^{-1} using a flow meter. According to the sample requirements for mass spectrometry pretreatment, we used deionized water as the absorption solution. A bubbler absorption bottle filled with absorption solution was used to collect NH_3 . Three atmospheric sam-

plers were operated simultaneously during each sampling event. Figure 1 marks the sampling points of the intensive pig farms with green pentagrams. Sampling was conducted in a typical commercial intensive laying-hen house with a conventional cage-based rearing system, representative of large-scale laying-hen farms in northern China. We collected gases from the exhaust vents of chicken houses and pig houses. These types of animal housing have centralized air inlets and outlets, so collecting from the exhaust vents can represent the ammonia emissions from these two types of housing into the atmosphere. For cattle farms, since the barns are open, we selected cattle sheds located in the middle of the farm to more effectively collect ammonia gas.

In the case of intensive laying hens farms, each building houses approximately 15 000 laying hens and is fully enclosed, with a total of 300 000 laying hens being raised. The sampling site is located in Zhengzhou City, Henan Province (114.03°E , 34.59°N). One building was selected as the target sampling point, with the sampling method mirroring that used for the fattening pig farms. As shown in Fig. 1, the light blue pentagons represent the sampling points of intensive layer farms.

The intensive dairy farm operates with an open-style barn design, housing 400 dairy cows per barn, with a total of 4000 dairy cows being raised. Four atmospheric samplers were installed in the passageways of the dairy barns, with each sampler spaced 10 m apart and positioned at a height of 1.6 m. The dairy farm is located in Zhengzhou City, Henan Province (114.11°E , 34.81°N). The sampling time and method remained consistent with those described above. In Fig. 1, the dark blue pentagons represent the sampling points of intensive dairy farms.

To investigate the variations in $\delta^{15}\text{N}$ levels associated with differing degrees of air pollution, samples collected for $\delta^{15}\text{N}$ measurement during periods of severe smog and when air quality was pristine. The sampling location was situated on a spacious lawn within the campus of Henan Agricultural University, devoid of tall buildings or traffic. The sampling point is illustrated in Fig. 1, where the pink triangle represents the sampling site for both haze and clean air (Longitude 113.82°E , Latitude 34.80°N). Each sampling event utilized three atmospheric samplers, positioned at a height of 1.6 m, with the duration of sampling aligned with that of the livestock farm.

The collected sample solution is transferred into a centrifuge tube and returned to the laboratory, where the concentration of NH_3 is measured using a UV spectrophotometer. The detection method adheres to the guidelines outlined in “Determination of Ammonia Nitrogen in Water by Salicylic Acid Spectrophotometry” (HJ 536-2009), and the calculation method is presented in Eq. (1):

$$\rho_N = \frac{A_s - A_b - a}{b \times V} \times D \quad (1)$$

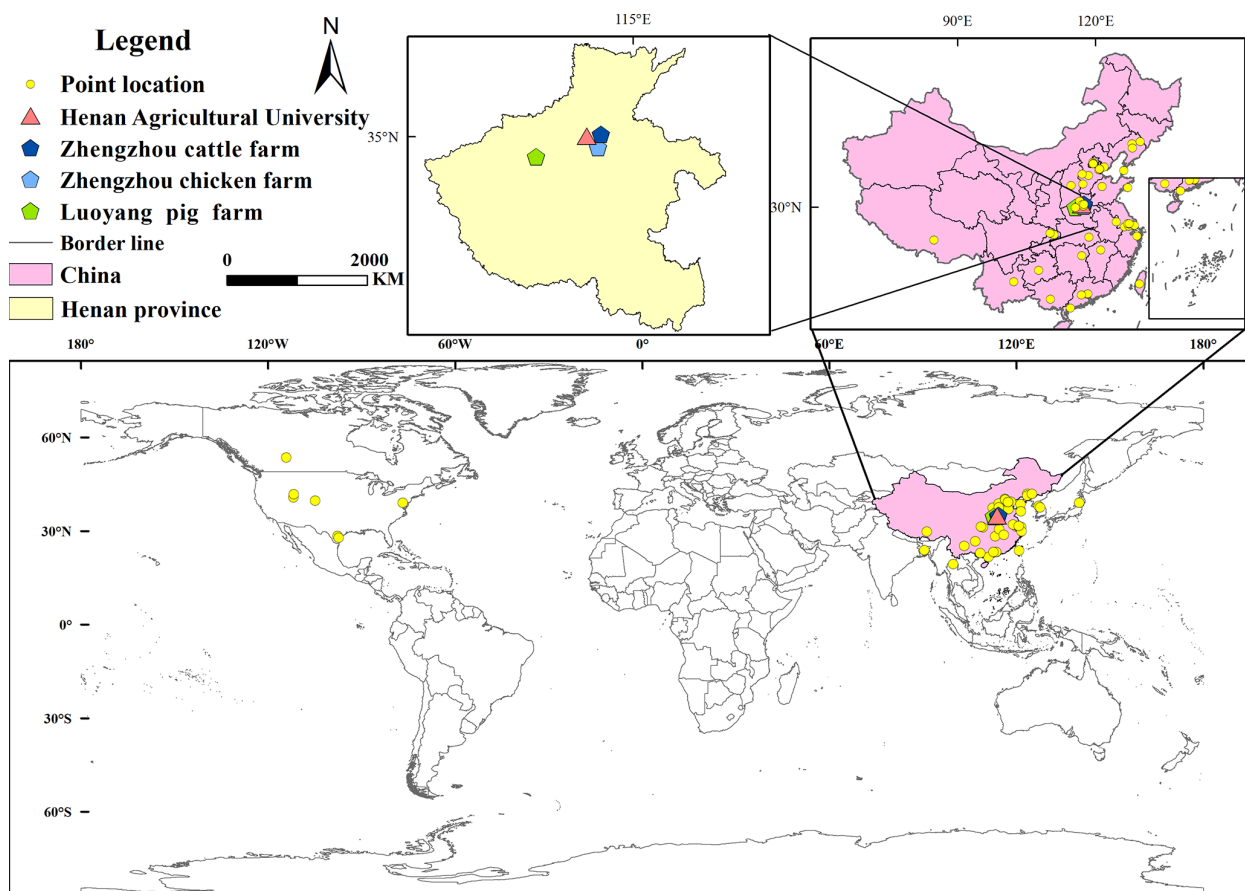


Figure 1. Sampling sites of livestock farms, haze weather, and clear weather in this study, extracted from the main research sampling locations. Yellow dots represent the main global research sampling sites, pink triangles represent sampling sites during haze and clear weather, dark blue pentagons represent cattle farms, light blue pentagons represent layer farms, and green pentagons represent fattening pig farms.

where, ρ_N represents the mass concentration of ammonia nitrogen in the water sample (expressed as N), in mg L^{-1} . The variables are defined as follows: A_s denotes the absorbance of the sample, while A_b indicates the absorbance of the blank experiment, which is prepared from the same batch as the sample. The parameters a and b correspond to the intercept and slope of the calibration curve, respectively. Additionally, V refers to the volume of the water sample taken, measured in mL, and D signifies the dilution factor of the water sample.

The analytical method for N isotope determination employs the hypobromite-hydroxylamine hydrochloride chemical method (Song et al., 2024) (Soler-Jofra et al., 2016; Zhang et al., 2007). Initially, a potassium bromate-potassium bromide solution reacts under acidic conditions to produce bromine, which subsequently reacts in a strongly alkaline environment to generate bromate, a potent oxidizing agent capable of oxidizing NH_4^+ to NO_2^- . In the following step, hydroxylamine hydrochloride reduces NO_2^- in an acidic environment to form N_2O . The resultant N_2O is then analyzed using a stable isotope ratio mass spectrometer, along with

a multi-purpose online gas preparation device, and an automatic sampler, to determine the $\delta^{15}\text{N}$ value. For each sample analysis, four international standard materials for NH_4^+ (IAEA-N-1, USGS-25, IAEA-N-2, and USGS-26, with $\delta^{15}\text{N}$ concentrations of 0.4‰, −30.41‰, 20.3‰, and 53.75‰, respectively) are processed simultaneously. NH_3 concentrations and $\delta^{15}\text{N}$ values are presented as mean \pm standard error (SE). Differences in $\delta^{15}\text{N}$ values among livestock categories were evaluated using one-way analysis of variance (ANOVA). When data did not meet the assumptions of normality or homogeneity of variance, non-parametric tests were applied. Statistical significance was defined at $p < 0.05$. All statistical analyses were conducted using standard statistical software.

2.2 Data collection and processing

We screened articles published between January 2000 and January 2025 regarding the sources of $\delta^{15}\text{N-NH}_3$ and $\delta^{15}\text{N-NH}_4^+$. Specifically, we utilized ISI Web of Science, Google Scholar, and PubMed, employing the search terms “ $\delta^{15}\text{N}$,”

“ NH_3 ,” “ammonia emissions,” and “isotopes” to identify relevant literature. Studies included in our analysis were required to meet the following criteria: (1) Samples must be measured for either $\delta^{15}\text{N-NH}_3$ or $\delta^{15}\text{N-NH}_4^+$; (2) Experiments must encompass at least one of the following: combustion, fertilization, agriculture, transportation, or livestock farming; (3) The number of experimental replicates and sampling events must be explicitly reported; (4) Samples must primarily consist of atmospheric NH_3 or $\text{PM}_{2.5}$, and detection must employ chemical methods. A total of 37 documents were included in the analysis. This dataset comprehensively encompasses multiple meta-analyses and original studies, detailing changes in $\delta^{15}\text{N-NH}_3$ and $\delta^{15}\text{N-NH}_4^+$ from combustion sources, transportation sources, agricultural sources, and livestock farming sources; the proportion of $\delta^{15}\text{N}$ values in the atmosphere; geographical location (latitude and longitude); and the GDP of each city where samples were collected. If the data in the literature was presented solely in chart form, we utilized WebPlotDigitizer-4.7 (<https://apps.automeris.io/wpd4/>, last access: 20 May 2025) to extract the data. We categorized the collected data into five distinct groups: combustion, transportation, farmland, livestock farming, and $\text{PM}_{2.5}$. To ensure reproducibility, literature-derived $\delta^{15}\text{N-NH}_3$ values were synthesized following a consistent aggregation protocol. When multiple isotopic values for the same source category were reported within a single study, a sample-size-weighted mean was calculated if the number of samples (n) was explicitly provided. In cases where sample size information was unavailable, simple arithmetic means were used, and the resulting uncertainty was reflected by expanding the reported end-member range. No additional weighting based on study duration or subjective data quality scores was applied, in order to avoid introducing implicit bias across studies. Differences between sampling methodologies were explicitly considered. Active sampling studies, including the present work, were prioritized for constraining source end-member values. Passive sampling data were used only for qualitative comparison, as previous studies have demonstrated systematic low biases in $\delta^{15}\text{N-NH}_3$ derived from passive samplers relative to active methods. Consequently, passive sampling results were not directly incorporated into end-member mean calculations used for isotope mixing analyses.

A total of 126 samples were collected, and 41 literature references were gathered. Data analysis was performed using Excel, SPSS, and Python version 3.11.

3 Result and discussion

3.1 Temporal Variations in Ammonia Emissions and $\delta^{15}\text{N}$ Signatures from Livestock Farms

During the sampling period from May to December, ammonia emissions varied significantly among the three farm types: 4.9 to 6.7 mg m^{-3} for fattening pigs (Fig. 2a), 1.7 and

2.5 mg m^{-3} for dairy cows (Fig. 2b), and 3.8 to 7.1 mg m^{-3} for laying hens (Fig. 2c), with the latter exhibiting substantial temporal fluctuations. NH_3 emissions from fattening pigs peaked when the pigs reached 130 kg per head (Fig. 2a). For laying hens, NH_3 concentrations initially increased and subsequently declined in response to temperature variations, reflecting enhanced urease activity within the housing environment, which accelerates urea hydrolysis and promotes NH_3 volatilization. $\delta^{15}\text{N-NH}_4^+$ levels at the livestock farms showed significant temporal variation ($p < 0.05$) (Groot Koerkamp et al., 1998; Rosa et al., 2020). From May to June, the $\delta^{15}\text{N-NH}_4^+$ increased from -31.0‰ to -25.2‰ in fattening pig farms and from -26.4‰ to -24.6‰ in laying hen farms. In September, $\delta^{15}\text{N-NH}_4^+$ values from fattening pig farms ($-13.3 \pm 1.3\text{‰}$) were significantly higher than those from laying hen and dairy cow farms ($-13.9 \pm 0.9\text{‰}$), which were comparable. Over the following three months, $\delta^{15}\text{N-NH}_4^+$ levels decreased significantly across both farm types. Although relatively large variability was observed within each livestock category, the differences in mean $\delta^{15}\text{N}$ values among groups were statistically significant (one-way ANOVA, $p < 0.05$). The large within-group variability reflects realistic operational and environmental heterogeneity and does not negate the statistically significant differences observed among livestock categories. As illustrated in Fig. 2, the highest NH_3 concentration at the dairy farm ($2.5 \pm 0.3 \text{ mg m}^{-3}$) occurred in October, coinciding with the lowest $\delta^{15}\text{N-NH}_4^+$ values, while laying hen farms also recorded minimum $\delta^{15}\text{N-NH}_4^+$ during this period of elevated NH_3 . Conversely, the lowest $\delta^{15}\text{N-NH}_4^+$ at fattening pig farms was observed in December, despite peak NH_3 concentrations. NH_3 concentrations differed significantly between hazy and clear weather in December (Fig. 2d), with $\delta^{15}\text{N-NH}_4^+$ values being significantly higher under clear conditions ($1.9 \pm 0.8\text{‰}$) than under hazy conditions ($1.6 \pm 0.2\text{‰}$; $p < 0.05$).

As illustrated in Fig. 3, throughout the entire monitoring period, ammonia (NH_3) sources from the farms exhibited nitrogen depletion, indicated by negative $\delta^{15}\text{N-NH}_4^+$ values. Overall, $\delta^{15}\text{N-NH}_4^+$ values exhibited significant fluctuations in dairy and fattening pig farms, while variations were comparatively moderate in laying hens farms. Notably, the $\delta^{15}\text{N-NH}_4^+$ values at dairy cattle farms displayed substantially greater overall changes during the monitoring period compared to those in laying hens and fattening pig farms. The arithmetic mean value at fattening pig farms was $-30.8 \pm 1.6\text{‰}$, the lowest among the three types of farms, whereas the $\delta^{15}\text{N-NH}_4^+$ values in laying hens manure remained at an intermediate level throughout the entire period. From October to December, the $\delta^{15}\text{N-NH}_4^+$ values at livestock and poultry farms were generally lower than those observed in the first half of the monitoring period (Fig. 3). However, when comparing hazy and clear weather conditions, the $\delta^{15}\text{N-NH}_4^+$ values for all three types of farms consistently remained at a relatively low level during this time-

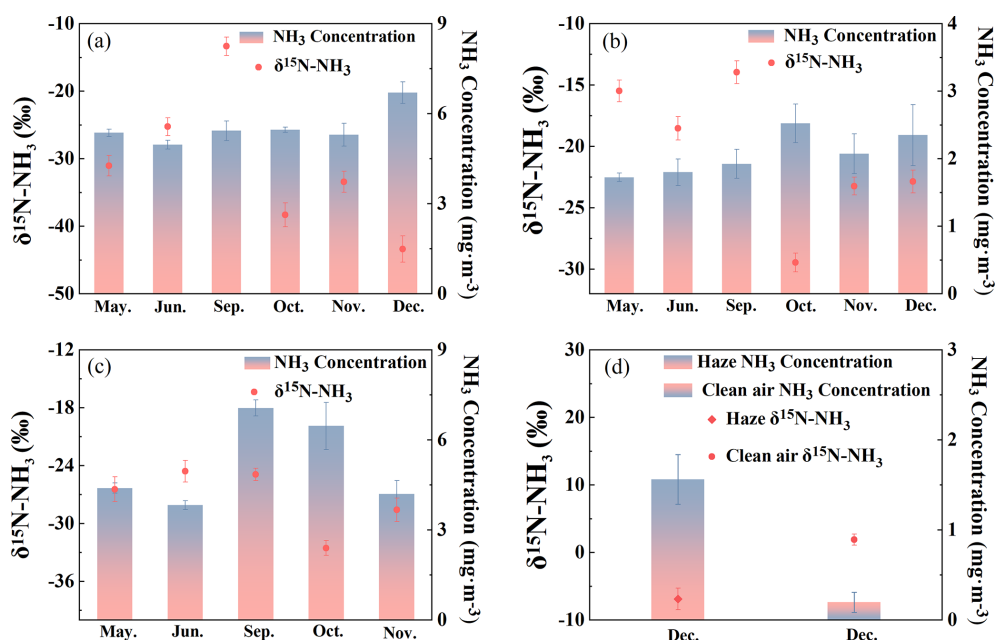


Figure 2. Changes in NH₃ emissions and $\delta^{15}\text{N-NH}_4^+$ values outside the livestock farms among different months. (a) Fattening pig farm; (b) Dairy cow farm; (c) Laying hens farm; (d) Comparison of Haze and clean air samples. Statistical difference was calculated by *t*-test, $p < 0.05$, $n = 3$.

frame (Fig. 3). High temperatures enhance enzyme activity and volatilization, thereby intensifying the isotopic fractionation effect during summer; whereas low temperatures inhibit these processes and reduce isotopic deviations. The nitrogen isotopic signature of livestock-derived ammonia is influenced by various biogeochemical processes, including urea hydrolysis during manure storage, microbial ammonification, and ammonia volatilization (Bhattarai and Wang, 2023; Huang et al., 2012; Li et al., 2023a).

3.2 Comparison with Literature and Implications for Local Sources

During the monitoring period, the $\delta^{15}\text{N-NH}_4^+$ values ranged from -50.0‰ to -10.0‰ (Fig. 4a). For fattening pigs, $\delta^{15}\text{N-NH}_4^+$ values averaged $-38.4\text{‰} \pm 1.8\text{‰}$ between October and December, which was significantly lower than the previously reported range of -27.10‰ to -31.7‰ (Chang et al., 2016). Notably, the overall variation remained within the $\delta^{15}\text{N-NH}_4^+$ emission ranges report for fattening pigs in other studies (Bhattarai and Wang, 2023; Wang et al., 2022). Furthermore, due to differences in livestock management practices and nitrogen content in feed, the $\delta^{15}\text{N-NH}_4^+$ values from dairy farms in this study, averaging $-29.4\text{‰} \pm 13.9\text{‰}$, were substantially lower than those reported by Martine et al. ($20.5\text{‰} \pm 34.5\text{‰}$) (Savard et al., 2017).

Comparison with $\delta^{15}\text{N-NH}_4^+$ values measured in dairy farms in Akita, Japan, were $-22.5\text{‰} \pm -14.6\text{‰}$ (Kawashima, 2019), no significant difference was observed relative to the values obtained in this study. However, these

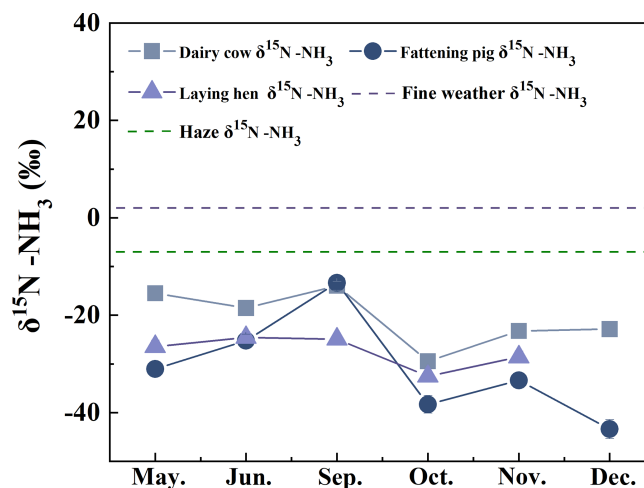


Figure 3. Changes of $\delta^{15}\text{N-NH}_4^+$ abundance at intensive livestock farms during the sampling period. Hazy and clean air were also sampled at December. The air sample of laying hens in December was missed, because of death of chicken by avian influenza.

values exceeded those reported by Felix et al. (2014), which ranged from -37.9‰ to -22.9‰ based on passive sampling techniques. Previous research has shown that active sampling generally yields higher $\delta^{15}\text{N}$ values than passive sampling (Kawashima and Ono, 2019; Pan et al., 2020). This discrepancy arises from the diffusion-driven nature of passive samplers, in which lighter NH₃ molecules are preferentially adsorbed. Consequently, passive sampling typically

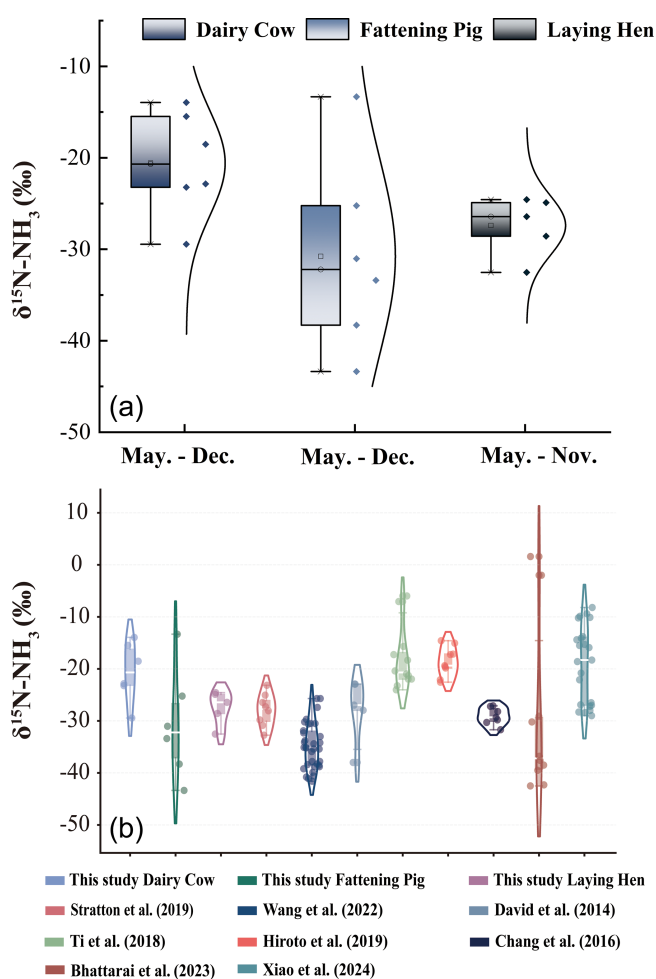


Figure 4. Comparison of $\delta^{15}\text{N-NH}_4^+$ values within different livestock farms and historical reported data. **(a)** Comparison of the $\delta^{15}\text{N-NH}_4^+$ values among different livestock farms; **(b)** Comparison of the $\delta^{15}\text{N-NH}_4^+$ values from present study with previously reported data. Boxes represent the interquartile range, the horizontal line within each box denotes the median value, and whiskers indicate the minimum and maximum values excluding outliers. Individual points outside the whiskers represent statistical outliers.

produces $\delta^{15}\text{N}$ values that deviate by approximately 15 ‰ from those obtained by active sampling (Bhattarai and Wang, 2023; Skinner et al., 2006). Variations in $\delta^{15}\text{N-NH}_4^+$ values are known to occur among different livestock species. During the monitoring period, $\delta^{15}\text{N-NH}_4^+$ values from laying hen farms were consistently lower than those from dairy farms but higher than those from fattening pig farms, consistent with previously reported trends (Liu et al., 2025; Ryu et al., 2021). This pattern suggests that $\delta^{15}\text{N-NH}_4^+$ variations in emitted NH_3 are not primarily driven by animal body weight but are instead strongly modulated by environmental conditions (Choi et al., 2017; Qu and Zhang, 2021). In agreement with earlier studies, $\delta^{15}\text{N-NH}_4^+$ emissions from fattening pig and laying hen farms differed significantly

from previously documented values, whereas no significant difference was observed for dairy cattle farms. Furthermore, the magnitude of $\delta^{15}\text{N-NH}_4^+$ fluctuations across the three farm types was smaller than that reported in earlier literature. Comparison with major atmospheric NH_3 sources further demonstrated that the $\delta^{15}\text{N-NH}_4^+$ values measured in this study diverged substantially from those associated with combustion ($-7.0\text{‰} \pm 2.1\text{‰}$), fertilization application ($-38.0\text{‰} \pm 0.2\text{‰}$), and transportation ($6.6\text{‰} \pm 2.1\text{‰}$). Based on $\delta^{15}\text{N-NH}_4^+$ signatures measured under both hazy and clear weather conditions, it can therefore be inferred that agricultural and livestock emissions are not the dominant contributors to atmospheric NH_3 in Zhengzhou. Instead, traffic exhaust and combustion sources appear to constitute the primary contributors. We conducted source apportionment for haze and clean weather using the MixSIAR model. The results showed that combustion and traffic were the main contributing sources, with combustion accounting for 29.0%, traffic for 38.0%, agriculture for 15.1%, and livestock for 17.8% (Stock and Semmens, 2016; Walters et al., 2022; Wong et al., 2022).

The selected pig, dairy, and laying hen facilities are typical of intensive livestock production systems in the southern Huang–Huai–Hai Plain, where feeding strategies, manure management, and ventilation designs are relatively standardized due to regional regulations and industrial practices. Previous studies have shown that while such operational differences can induce secondary variability in $\delta^{15}\text{N}$ signatures, their influence is generally smaller than the systematic isotopic contrasts observed among different livestock species.

Importantly, the objective of this study is not to characterize farm-to-farm variability, but to constrain representative isotopic end-member ranges for major livestock categories that can be applied in regional source apportionment frameworks. Within this context, the internally consistent sampling protocol and the clear separation of $\delta^{15}\text{N-NH}_4^+$ values among livestock types suggest that the derived signatures are robust for intensive livestock systems operating under comparable management conditions (Choi et al., 2017; Parnell et al., 2010).

Extrapolation of these $\delta^{15}\text{N}$ signatures beyond the studied region or to non-standardized, small-scale, or pasture-based livestock systems should be undertaken with caution. Future work incorporating multiple facilities per livestock type and explicit characterization of feed and ventilation parameters would further refine the regional representativeness of livestock-derived ammonia isotope signatures.

3.3 Global Variability of NH_3 Source Signatures and Challenges for Source Apportionment

Ammonia emissions that contribute to urban smog primarily arise from combustion activities, vehicle exhaust, agriculture fertilization, and livestock production. As national economies expand, the frequency and severity of smog

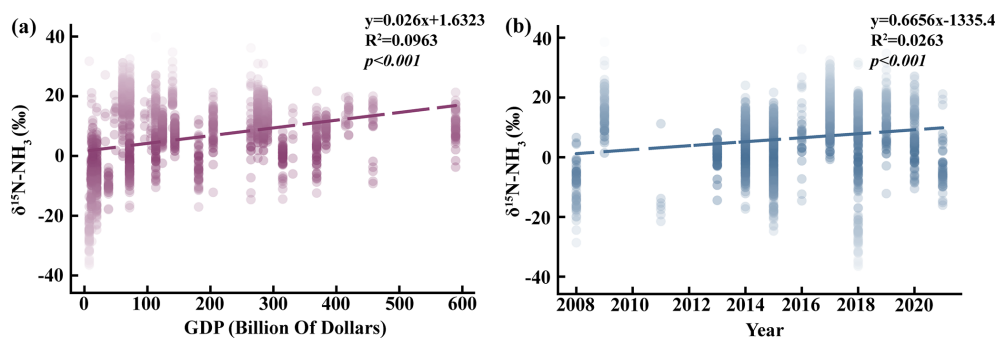


Figure 5. Changes of $\delta^{15}\text{N-NH}_4^+$ values among different GDP cities and years. (a) The relationship between GDP and $\delta^{15}\text{N-NH}_4^+$ values ($p < 0.001$); (b) Changes of $\delta^{15}\text{N-NH}_4^+$ values reported between 2008 to 2021 ($p < 0.001$).

events have intensified. Figure 5a (slope: 0.026, intercept: 1.6323, R^2 : 0.0963) shows that from 2000 to 2025, when GDP remains below USD 70 billion, atmospheric $\delta^{15}\text{N-NH}_4^+$ signatures predominantly reflect fertilizer-derived emissions from agricultural regions and NH_3 volatilization from livestock operations (Kawashima et al., 2022; Kawashima and Kurahashi, 2011). This pattern indicates that lower-income regions rely heavily on agriculture and animal husbandry as the foundational components of their economies (Leng et al., 2018).

When GDP increases to between USD 80 and 300 billion, the contribution of combustion-related and vehicular sources to $\delta^{15}\text{N-NH}_4^+$ becomes increasingly prominent. Notably, vehicle exhaust remains the dominant contributor within this GDP interval, suggesting that transportation serves as a key economic driver during mid-stage development. In densely populated and economically advanced cities, rapid vehicle growth further amplifies the influence of transportation-related $\delta^{15}\text{N-NH}_4^+$ signatures (Lim et al., 2022; Pan et al., 2018; Stratton et al., 2019). Throughout the entire dataset, vehicle exhaust and combustion together account for nearly 70 % of ammonia emissions (Wu et al., 2019). Once GDP surpasses 300 billion USD, $\delta^{15}\text{N-NH}_4^+$ from combustion becomes the dominant atmospheric source, while the relative contribution from vehicle exhaust begins to decline and emissions from agricultural fertilization and livestock farming become negligible (Li et al., 2023b). It is important to note that sampling sites in the present study were located near power plants (Lim et al., 2019; Zou et al., 2022), whereas comparison data from previous studies were collected in urban cores. This spatial difference further supports the conclusion that in highly developed cities, shifts in economic structure lead to combustion sources emerging as the principal contributors to atmospheric NH_3 under both hazy and clear meteorological conditions. As illustrated in Fig. 5b, the proportion of $\delta^{15}\text{N-NH}_4^+$ attributed to combustion and vehicular sources has increased over time. This temporal trend suggests that, with economic growth, agricultural and livestock emissions

no longer represent the dominant contributors to atmospheric ammonia.

The extracted dataset was classified into four major emission categories—livestock farming, combustion, farmland fertilization, and vehicle exhaust—and subsequently subjected to statistical evaluation. As illustrated in Fig. 6, $\delta^{15}\text{N-NH}_4^+$ values associated with combustion sources showed strong consistency with previously reported ranges (Chang et al., 2021). Although traffic exhaust and livestock-related $\delta^{15}\text{N-NH}_4^+$ values exhibited moderate dispersion, both sources remained within relatively well-defined isotopic ranges. In sharp contrast, $\delta^{15}\text{N-NH}_4^+$ signatures following farmland fertilization displayed pronounced heterogeneity, covering nearly the entire isotopic spectrum reported for combustion, livestock, and vehicular emissions. This extensive variability highlights substantial regional differences in agricultural ammonia emission processes (Felix et al., 2014; Li et al., 2023b). Consequently, accurate source apportionment of atmospheric NH_3 requires distinguishing dominant local emission pathways rather than relying solely on generalized isotopic patterns (Chen et al., 2022; Zhang et al., 2023).

4 Summary

This study establishes high-precision $\delta^{15}\text{N}$ signatures for ammonia emissions from three dominant intensive livestock systems in the Huang-Huai-Hai Plain. Distinct isotopic fingerprints were identified for dairy operations ($-20.6\text{‰} \pm 0.8\text{‰}$), laying hen facilities ($-27.4\text{‰} \pm 1.0\text{‰}$), and fattening pig farms ($-38.4\text{‰} \pm 1.7\text{‰}$), underscoring clear differences among livestock categories. Our results further demonstrate that isotopic signatures vary dynamically with NH_3 volatilization intensity, highlighting the need to incorporate volatilization-driven fractionation effects into isotope-based source apportionment frameworks. When compared with ambient $\delta^{15}\text{N-NH}_4^+$ measurements in Zhengzhou, the newly constrained source end-members indicate that non-agricultural sources—particularly vehicular emissions and combustion—are

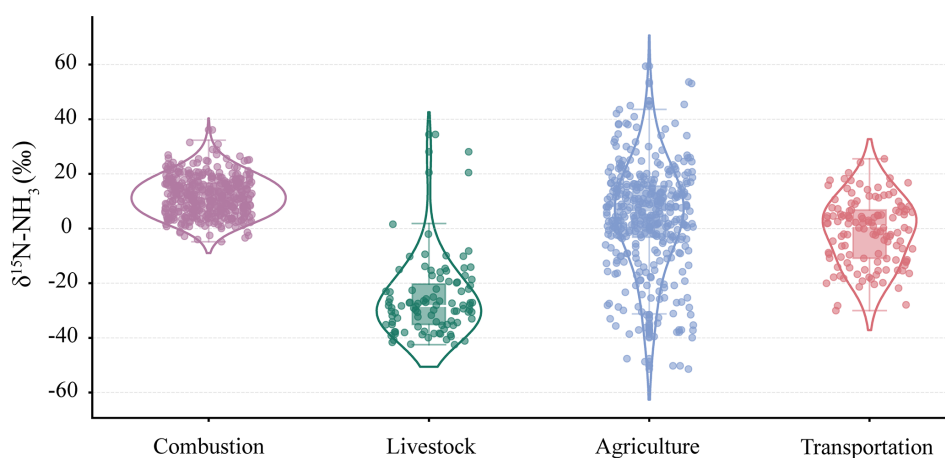


Figure 6. Statistical analysis of extracted data categorized by source: combustion sources, livestock and poultry farming sources, agricultural sources, and transportation exhaust sources. Boxes represent the interquartile range, the horizontal line within each box denotes the median value, and whiskers indicate the minimum and maximum values excluding outliers. Individual points outside the whiskers represent statistical outliers.

likely major contributors to urban atmospheric ammonia. This interpretation, however, requires validation through comprehensive isotopic mixing and dispersion modeling. Moreover, global-scale evaluation reveals that the exceptional variability of $\delta^{15}\text{N}$ associated with fertilized soils continues to pose a substantial challenge for accurate identification of agricultural contributions. Collectively, the findings presented here provide critical isotopic constraints that can enhance regional atmospheric chemistry models and support the design of more precise and effective ammonia emission control policies.

Data availability. All datasets used in this study are publicly available on Zenodo (<https://doi.org/10.5281/ZENODO.17639507>, Wang et al., 2025). The data underlying Figs. 1–6 are included in this repository. Key results are presented in Sects. 3–4 of the main text.

Supplement. The supplement related to this article is available online at <https://doi.org/10.5194/acp-26-4953-2026-supplement>.

Author contributions. JW – Drafting, Formal Analysis, Data Management, Methodology, Investigation; ZN – Formal Analysis, Data Management, Methodology, Investigation; YZ – Conceptualization, Data Management, Visualization, Funding Acquisition, Drafting, Formal Analysis, Writing – Review and Editing; XJ – Data Management, Visualization; HaL – Data Management, Methodology; PZ – Formal Analysis, Data Management; HoL – Writing – Review and Editing, Funding Acquisition, Conceptualization, Supervision.

Competing interests. The contact author has declared that none of the authors has any competing interests.

Disclaimer. Publisher’s note: Copernicus Publications remains neutral with regard to jurisdictional claims made in the text, published maps, institutional affiliations, or any other geographical representation in this paper. The authors bear the ultimate responsibility for providing appropriate place names. Views expressed in the text are those of the authors and do not necessarily reflect the views of the publisher.

Acknowledgements. This research was supported by the National Key Research and Development Program of China (2021 YFD 1700900), the Industrial Technology System for Cultivated Land Protection in Henan Province (HARS-22-19-S), the Natural Science Foundation of Henan Province (grant no. 252300420043), and the Key Research and Development Program of Henan Province (grant no. 25111112200).

Financial support. This research was supported by the National Key Research and Development Program of China (2021 YFD 1700900), the Industrial Technology System for Cultivated Land Protection in Henan Province (HARS-22-19-S), the Natural Science Foundation of Henan Province (grant no. 252300420043), and the Key Research and Development Program of Henan Province (grant no. 25111112200).

Review statement. This paper was edited by Tao Wang and reviewed by two anonymous referees.

References

- Battye, W.: Evaluation and improvement of ammonia emissions inventories, *Atmos. Environ.*, 37, 3873–3883, [https://doi.org/10.1016/S1352-2310\(03\)00343-1](https://doi.org/10.1016/S1352-2310(03)00343-1), 2003.
- Berner, A. H. and David Felix, J.: Investigating ammonia emissions in a coastal urban airshed using stable isotope techniques, *Sci. Total Environ.*, 707, 134952, <https://doi.org/10.1016/j.scitotenv.2019.134952>, 2020.
- Beusen, A. H. W., Bouwman, A. F., Heuberger, P. S. C., Van Drecht, G., and Van Der Hoek, K. W.: Bottom-up uncertainty estimates of global ammonia emissions from global agricultural production systems, *Atmos. Environ.*, 42, 6067–6077, <https://doi.org/10.1016/j.atmosenv.2008.03.044>, 2008.
- Bhattacharai, N. and Wang, S.: Active vs. passive isotopic analysis: insights from urban beijing field measurements and ammonia source signatures, *Atmos. Environ.*, 314, 120079, <https://doi.org/10.1016/j.atmosenv.2023.120079>, 2023.
- Bhattacharai, N., Wang, S., Xu, Q., Dong, Z., Chang, X., Jiang, Y., and Zheng, H.: Sources of gaseous NH_3 in urban beijing from parallel sampling of NH_3 and NH_4^+ , their nitrogen isotope measurement and modeling, *Sci. Total Environ.*, 747, 141361, <https://doi.org/10.1016/j.scitotenv.2020.141361>, 2020.
- Bouwman, A. F., Lee, D. S., Asman, W. A. H., Dentener, F. J., Van Der Hoek, K. W., and Olivier, J. G. J.: A global high-resolution emission inventory for ammonia, *Global Biogeochem. Cy.*, 11, 561–587, <https://doi.org/10.1029/97GB02266>, 1997.
- Boyle, E.: Nitrogen pollution knows no bounds, *Science*, 356, 700–701, <https://doi.org/10.1126/science.aan3242>, 2017.
- Chang, Y., Liu, X., Deng, C., Dore, A. J., and Zhuang, G.: Source apportionment of atmospheric ammonia before, during, and after the 2014 APEC summit in Beijing using stable nitrogen isotope signatures, *Atmos. Chem. Phys.*, 16, 11635–11647, <https://doi.org/10.5194/acp-16-11635-2016>, 2016.
- Chang, Y., Zhang, Y.-L., Kawichai, S., Wang, Q., Van Damme, M., Clarisse, L., Prapamontol, T., and Lehmann, M. F.: Convergent evidence for the pervasive but limited contribution of biomass burning to atmospheric ammonia in peninsular Southeast Asia, *Atmos. Chem. Phys.*, 21, 7187–7198, <https://doi.org/10.5194/acp-21-7187-2021>, 2021.
- Chen, T.-Y., Chen, C.-L., Chen, Y.-C., Chou, C. C.-K., Ren, H., and Hung, H.-M.: Source apportionment and evolution of N-containing aerosols at a rural cloud forest in Taiwan by isotope analysis, *Atmos. Chem. Phys.*, 22, 13001–13012, <https://doi.org/10.5194/acp-22-13001-2022>, 2022.
- Choi, W.-J., Kwak, J.-H., Lim, S.-S., Park, H.-J., Chang, S. X., Lee, S.-M., Arshad, M. A., Yun, S.-I., and Kim, H.-Y.: Synthetic fertilizer and livestock manure differently affect $\delta^{15}\text{N}$ in the agricultural landscape: a review, *Agric. Ecosyst. Environ.*, 237, 1–15, <https://doi.org/10.1016/j.agee.2016.12.020>, 2017.
- Elliott, E. M., Yu, Z., Cole, A. S., and Coughlin, J. G.: Isotopic advances in understanding reactive nitrogen deposition and atmospheric processing, *Sci. Total Environ.*, 662, 393–403, <https://doi.org/10.1016/j.scitotenv.2018.12.177>, 2019.
- Felix, J. D., Elliott, E. M., Gish, T., Maghirang, R., Cambal, L., and Clougherty, J.: Examining the transport of ammonia emissions across landscapes using nitrogen isotope ratios, *Atmos. Environ.*, 95, 563–570, <https://doi.org/10.1016/j.atmosenv.2014.06.061>, 2014.
- Ferm, M.: Method for determination of atmospheric ammonia, *Atmos. Environ.* 1967, 13, 1385–1393, [https://doi.org/10.1016/0004-6981\(79\)90107-0](https://doi.org/10.1016/0004-6981(79)90107-0), 1979.
- Goebes, M. D., Strader, R., and Davidson, C.: An ammonia emission inventory for fertilizer application in the United States, *Atmos. Environ.*, 37, 2539–2550, [https://doi.org/10.1016/S1352-2310\(03\)00129-8](https://doi.org/10.1016/S1352-2310(03)00129-8), 2003.
- Groot Koerkamp, P. W. G., Metz, J. H. M., Uenk, G. H., Phillips, V. R., Holden, M. R., Sneath, R. W., Short, J. L., White, R. P. P., Hartung, J., Seedorf, J., Schröder, M., Linkert, K. H., Pedersen, S., Takai, H., Johnsen, J. O., and Wathes, C. M.: Concentrations and emissions of ammonia in livestock buildings in northern Europe, *J. Agric. Eng. Res.*, 70, 79–95, <https://doi.org/10.1006/jaer.1998.0275>, 1998.
- Harrison, R. M. and Kitto, A.-M. N.: Field intercomparison of filter pack and denuder sampling methods for reactive gaseous and particulate pollutants, *Atmos. Environ.*, 24, 2633–2640, [https://doi.org/10.1016/0960-1686\(90\)90142-A](https://doi.org/10.1016/0960-1686(90)90142-A), 1990.
- Heaton, T. H. E.: Isotopic studies of nitrogen pollution in the hydrosphere and atmosphere: a review, *Chem. Geol. Isot. Geosci. Sect.*, 59, 87–102, [https://doi.org/10.1016/0168-9622\(86\)90059-X](https://doi.org/10.1016/0168-9622(86)90059-X), 1986.
- Hristov, A. N., Zaman, S., Vander Pol, M., Ndegwa, P., Campbell, L., and Silva, S.: Nitrogen losses from dairy manure estimated through nitrogen mass balance and chemical markers, *J. Environ. Qual.*, 38, 2438–2448, <https://doi.org/10.2134/jeq2009.0057>, 2009.
- Huang, R.-J., Zhang, Y., Bozzetti, C., Ho, K.-F., Cao, J.-J., Han, Y., Daellenbach, K. R., Slowik, J. G., Platt, S. M., Canonaco, F., Zotter, P., Wolf, R., Pieber, S. M., Bruns, E. A., Crippa, M., Ciarelli, G., Piazzalunga, A., Schwikowski, M., Abbaszade, G., Schnelle-Kreis, J., Zimmermann, R., An, Z., Szidat, S., Baltensperger, U., Haddad, I. E., and Prévôt, A. S. H.: High secondary aerosol contribution to particulate pollution during haze events in China, *Nature*, 514, 218–222, <https://doi.org/10.1038/nature13774>, 2014.
- Huang, X., Song, Y., Li, M., Li, J., Huo, Q., Cai, X., Zhu, T., Hu, M., and Zhang, H.: A high-resolution ammonia emission inventory in China, *Global Biogeochem. Cy.*, 26, 2011GB004161, <https://doi.org/10.1029/2011GB004161>, 2012.
- Jiang, H., Zhang, Q., Liu, W., Zhang, J., Pan, K., Zhao, T., and Xu, Z.: Isotopic compositions reveal the driving forces of high nitrate level in an urban river: implications for pollution control, *J. Clean. Prod.*, 298, 126693, <https://doi.org/10.1016/j.jclepro.2021.126693>, 2021.
- Kawashima, H.: Seasonal trends of the stable nitrogen isotope ratio in particulate nitrogen compounds and their gaseous precursors in Akita, Japan, *Tellus Ser. B*, 71, <https://doi.org/10.1080/16000889.2019.1627846>, 2019.
- Kawashima, H. and Kurahashi, T.: Inorganic ion and nitrogen isotopic compositions of atmospheric aerosols at yurihonjo, *Atmos. Environ.*, 45, 6309–6316, <https://doi.org/10.1016/j.atmosenv.2011.08.057>, 2011.
- Kawashima, H. and Ono, S.: Nitrogen isotope fractionation from ammonia gas to ammonium in particulate ammonium chloride, *Environ. Sci. Technol.*, 53, 10629–10635, <https://doi.org/10.1021/acs.est.9b01569>, 2019.
- Kawashima, H., Yoshida, O., Joy, K. S., Raju, R. A., Islam, K. N., Jeba, F., and Salam, A.: Sources identification of ammonium in $\text{PM}_{2.5}$ during monsoon season in Dhaka, Bangladesh, *Sci. Total Environ.*, 514, 218–222, <https://doi.org/10.1038/nature13774>, 2014.

- Environ., 838, <https://doi.org/10.1016/j.scitotenv.2022.156433>, 2022.
- Kawashima, H., Yoshida, O., and Suto, N.: Long-term source apportionment of ammonium in $\text{PM}_{2.5}$ at a suburban and a rural site using stable nitrogen isotopes, *Environ. Sci. Technol.*, 57, 1268–1277, <https://doi.org/10.1021/acs.est.2c06311>, 2023.
- Kirkby, J., Curtius, J., Almeida, J., Dunne, E., Duplissy, J., Ehrhart, S., Franchin, A., Gagné, S., Ickes, L., Kürten, A., Kupc, A., Metzger, A., Riccobono, F., Rondo, L., Schobesberger, S., Tsagko-georgas, G., Wimmer, D., Amorim, A., Bianchi, F., Breitenlechner, M., David, A., Dommen, J., Downard, A., Ehn, M., Flanagan, R. C., Haider, S., Hansel, A., Hauser, D., Jud, W., Junninen, H., Kreissl, F., Kvashin, A., Laaksonen, A., Lehtipalo, K., Lima, J., Lovejoy, E. R., Makhmutov, V., Mathot, S., Mikkilä, J., Minginette, P., Mogo, S., Nieminen, T., Onnela, A., Pereira, P., Petäjä, T., Schnitzhofer, R., Seinfeld, J. H., Sipilä, M., Stozhkov, Y., Stratmann, F., Tomé, A., Vanhanen, J., Viisanen, Y., Vrtala, A., Wagner, P. E., Walther, H., Weingartner, E., Wex, H., Winkler, P. M., Carslaw, K. S., Worsnop, D. R., Baltensperger, U., and Kulmala, M.: Role of sulphuric acid, ammonia and galactic cosmic rays in atmospheric aerosol nucleation, *Nature*, 476, 429–433, <https://doi.org/10.1038/nature10343>, 2011.
- Leng, Q., Cui, J., Zhou, F., Du, K., Zhang, L., Fu, C., Liu, Y., Wang, H., Shi, G., Gao, M., Yang, F., and He, D.: Wet-only deposition of atmospheric inorganic nitrogen and associated isotopic characteristics in a typical mountain area, southwestern China, *Sci. Total Environ.*, 616, 55–63, <https://doi.org/10.1016/j.scitotenv.2017.10.240>, 2018.
- Li, K., Xu, D., Zhang, L., Liu, W., Zhan, M., Su, Y., Wu, D., and Xie, B.: Integrated isotopic labeling analysis unveils precise proportions of ammonia emissions during composting, *J. Clean. Prod.*, 450, 141799, <https://doi.org/10.1016/j.jclepro.2024.141799>, 2024.
- Li, T., Wang, C., Ji, W., Wang, Z., Shen, W., Feng, Y., and Zhou, M.: Cutting-edge ammonia emissions monitoring technology for sustainable livestock and poultry breeding: a comprehensive review of the state of the art, *J. Clean. Prod.*, 428, 139387, <https://doi.org/10.1016/j.jclepro.2023.139387>, 2023a.
- Li, T., Li, J., Sun, Z., Jiang, H., Tian, C., and Zhang, G.: High contribution of anthropogenic combustion sources to atmospheric inorganic reactive nitrogen in South China evidenced by isotopes, *Atmos. Chem. Phys.*, 23, 6395–6407, <https://doi.org/10.5194/acp-23-6395-2023>, 2023b.
- Lim, S., Lee, M., Czimeczik, C. I., Joo, T., Holden, S., Mouteva, G., Santos, G. M., Xu, X., Walker, J., Kim, S., Kim, H. S., Kim, S., and Lee, S.: Source signatures from combined isotopic analyses of $\text{PM}_{2.5}$ carbonaceous and nitrogen aerosols at the peri-urban taehwa research forest, south Korea in summer and fall, *Sci. Total Environ.*, 655, 1505–1514, <https://doi.org/10.1016/j.scitotenv.2018.11.157>, 2019.
- Lim, S., Hwang, J., Lee, M., Czimeczik, C. I., Xu, X., and Savarino, J.: Robust evidence of ^{14}C , ^{13}C , and ^{15}N analyses indicating fossil fuel sources for total carbon and ammonium in fine aerosols in Seoul megacity, *Environ. Sci. Technol.*, 56, 6894–6904, <https://doi.org/10.1021/acs.est.1c03903>, 2022.
- Liu, D., Quan, Z., Wang, Y., Huang, K., Zhang, Q., Song, L., Huang, S., Wang, Y., Xun, Z., Liu, D., Liu, C., Fang, Y., and Sun, J.: Investigating the effects of animal-specific $\delta^{15}\text{N}\text{-NH}_3$ values volatilized from livestock waste on regional NH_3 source partitioning, *Atmospheric Environ. X*, 25, 100314, <https://doi.org/10.1016/j.aeaoa.2025.100314>, 2025.
- Liu, M., Huang, X., Song, Y., Tang, J., Cao, J., Zhang, X., Zhang, Q., Wang, S., Xu, T., Kang, L., Cai, X., Zhang, H., Yang, F., Wang, H., Yu, J. Z., Lau, A. K. H., He, L., Huang, X., Duan, L., Ding, A., Xue, L., Gao, J., Liu, B., and Zhu, T.: Ammonia emission control in China would mitigate haze pollution and nitrogen deposition, but worsen acid rain, *P. Natl. Acad. Sci. USA*, 116, 7760–7765, <https://doi.org/10.1073/pnas.1814880116>, 2019.
- Liu, X., Zhang, Y., Han, W., Tang, A., Shen, J., Cui, Z., Vitousek, P., Erisman, J. W., Goulding, K., Christie, P., Fangmeier, A., and Zhang, F.: Enhanced nitrogen deposition over China, *Nature*, 494, 459–462, <https://doi.org/10.1038/nature11917>, 2013.
- Ma, R., Zou, J., Han, Z., Yu, K., Wu, S., Li, Z., Liu, S., Niu, S., Horwath, W. R., and Zhu-Barker, X.: Global soil-derived ammonia emissions from agricultural nitrogen fertilizer application: a refinement based on regional and crop-specific emission factors, *Glob. Change Biol.*, 27, 855–867, <https://doi.org/10.1111/gcb.15437>, 2021.
- Meng, W., Zhong, Q., Yun, X., Zhu, X., Huang, T., Shen, H., Chen, Y., Chen, H., Zhou, F., Liu, J., Wang, X., Zeng, E. Y., and Tao, S.: Improvement of a global high-resolution ammonia emission inventory for combustion and industrial sources with new data from the residential and transportation sectors, *Environ. Sci. Technol.*, 51, 2821–2829, <https://doi.org/10.1021/acs.est.6b03694>, 2017.
- Pan, Y., Tian, S., Liu, D., Fang, Y., Zhu, X., Gao, M., Wentworth, G. R., Michalski, G., Huang, X., and Wang, Y.: Source apportionment of aerosol ammonium in an ammonia-rich atmosphere: an isotopic study of summer clean and hazy days in urban Beijing, *J. Geophys. Res.-Atmos.*, 123, 5681–5689, <https://doi.org/10.1029/2017JD028095>, 2018.
- Pan, Y., Gu, M., Song, L., Tian, S., Wu, D., Walters, W. W., Yu, X., Lü, X., Ni, X., Wang, Y., Cao, J., Liu, X., Fang, Y., and Wang, Y.: Systematic low bias of passive samplers in characterizing nitrogen isotopic composition of atmospheric ammonia, *Atmos. Res.*, 243, 105018–105025, <https://doi.org/10.1016/j.atmosres.2020.105018>, 2020.
- Parnell, A. C., Inger, R., Bearhop, S., and Jackson, A. L.: Source partitioning using stable isotopes: coping with too much variation, *PLOS One*, 5, e9672, <https://doi.org/10.1371/journal.pone.0009672>, 2010.
- Qu, Q. and Zhang, K.: Effects of pH, total solids, temperature and storage duration on gas emissions from slurry storage: a systematic review, *Atmosphere*, 12, 1156, <https://doi.org/10.3390/atmos12091156>, 2021.
- Rosa, E., Arriaga, H., and Merino, P.: Ammonia emission from a manure-belt laying hen facility equipped with an external manure drying tunnel, *J. Clean. Prod.*, 251, 119591, <https://doi.org/10.1016/j.jclepro.2019.119591>, 2020.
- Ryu, H.-D., Kim, S.-J., Baek, U., Kim, D.-W., Lee, H.-J., Chung, E. G., Kim, M.-S., Kim, K., and Lee, J. K.: Identifying nitrogen sources in intensive livestock farming watershed with swine excreta treatment facility using dual ammonium ($\delta^{15}\text{N}\text{NH}_4$) and nitrate ($\delta^{15}\text{N}\text{NO}_3$) nitrogen isotope ratios axes, *Sci. Total Environ.*, 779, 146480, <https://doi.org/10.1016/j.scitotenv.2021.146480>, 2021.
- Savard, M. M., Cole, A., Smirnov, A., and Vet, R.: $\delta^{15}\text{N}$ values of atmospheric N species simultaneously collected

- using sector-based samplers distant from sources – isotopic inheritance and fractionation, *Atmos. Environ.*, 162, 11–22, <https://doi.org/10.1016/j.atmosenv.2017.05.010>, 2017.
- Schlesinger, W. H. and Hartley, A. E.: A global budget for atmospheric NH_3 , *Biogeochemistry*, 15, <https://doi.org/10.1007/bf00002936>, 1992.
- Skinner, R., Ineson, P., Jones, H., Sleep, D., and Theobald, M.: Sampling systems for isotope-ratio mass spectrometry of atmospheric ammonia, *Rapid Commun. Mass Spectrom.*, 20, 81–88, <https://doi.org/10.1002/rcm.2279>, 2006.
- Soler-Jofra, A., Stevens, B., Hoekstra, M., Picioreanu, C., Sorokin, D., Van Loosdrecht, M. C. M., and Pérez, J.: Importance of abiotic hydroxylamine conversion on nitrous oxide emissions during nitrification of reject water, *Chem. Eng. J.*, 287, 720–726, <https://doi.org/10.1016/j.cej.2015.11.073>, 2016.
- Song, L., Walters, W. W., Pan, Y., Li, Z., Gu, M., Duan, Y., Lü, X., and Fang, Y.: ^{15}N natural abundance of vehicular exhaust ammonia, quantified by active sampling techniques, *Atmos. Environ.*, 255, 118430–118440, <https://doi.org/10.1016/j.atmosenv.2021.118430>, 2021.
- Song, L., Wang, A., Li, Z., Kang, R., Walters, W. W., Pan, Y., Quan, Z., Huang, S., and Fang, Y.: Large seasonal variation in nitrogen isotopic abundances of ammonia volatilized from a cropland ecosystem and implications for regional NH_3 source partitioning, *Environ. Sci. Technol.*, 58, 1177–1186, <https://doi.org/10.1021/acs.est.3c08800>, 2024.
- Stock, B. C. and Semmens, B. X.: Unifying error structures in commonly used biotracer mixing models, *Ecology*, 97, 2562–2569, <https://doi.org/10.1002/ecy.1517>, 2016.
- Stratton, J. J., Ham, J., Collett, J. L., Jr., Benedict, K., and Borch, T.: Assessing the efficacy of nitrogen isotopes to distinguish colorado front range ammonia sources affecting rocky mountain national park, *Atmos. Environ.*, 215, <https://doi.org/10.1016/j.atmosenv.2019.116881>, 2019.
- Streets, D. G., Bond, T. C., Carmichael, G. R., Fernandes, S. D., Fu, Q., He, D., Klimont, Z., Nelson, S. M., Tsai, N. Y., Wang, M. Q., Woo, J.-H., and Yarber, K. F.: An inventory of gaseous and primary aerosol emissions in Asia in the year 2000, *J. Geophys. Res.-Atmos.*, 108, <https://doi.org/10.1029/2002JD003093>, 2003.
- Sui, Y., Ou, Y., Yan, B., Rousseau, A. N., Fang, Y., Geng, R., Wang, L., and Ye, N.: A dual isotopic framework for identifying nitrate sources in surface runoff in a small agricultural watershed, northeast China, *J. Clean. Prod.*, 246, 119074, <https://doi.org/10.1016/j.jclepro.2019.119074>, 2020.
- Ti, C., Gao, B., Luo, Y., Wang, X., Wang, S., and Yan, X.: Isotopic characterization of $\text{NH}_x\text{-N}$ in deposition and major emission sources, *Biogeochemistry*, 138, 85–102, <https://doi.org/10.1007/s10533-018-0432-3>, 2018.
- Ti, C., Xia, L., Chang, S. X., and Yan, X.: Potential for mitigating global agricultural ammonia emission: A meta-analysis, *Environ. Pollut.*, 245, 141–148, <https://doi.org/10.1016/j.envpol.2018.10.124>, 2019.
- Ti, C., Ma, S., Peng, L., Tao, L., Wang, X., Dong, W., Wang, L., and Yan, X.: Changes of $\delta^{15}\text{N}$ values during the volatilization process after applying urea on soil, *Environ. Pollut.*, 270, 116204, <https://doi.org/10.1016/j.envpol.2020.116204>, 2021.
- Van Damme, M., Clarisse, L., Whitburn, S., Hadji-Lazaro, J., Hurtmans, D., Clerbaux, C., and Coheur, P.-F.: Industrial and agricultural ammonia point sources exposed, *Nature*, 564, 99–103, <https://doi.org/10.1038/s41586-018-0747-1>, 2018.
- Walters, W. W., Karod, M., Willcocks, E., Baek, B. H., Blum, D. E., and Hastings, M. G.: Quantifying the importance of vehicle ammonia emissions in an urban area of northeastern USA utilizing nitrogen isotopes, *Atmos. Chem. Phys.*, 22, 13431–13448, <https://doi.org/10.5194/acp-22-13431-2022>, 2022.
- Wang, C., Yin, S., Bai, L., Zhang, X., Gu, X., Zhang, H., Lu, Q., and Zhang, R.: High-resolution ammonia emission inventories with comprehensive analysis and evaluation in Henan, China, 2006–2016, *Atmos. Environ.*, 193, 11–23, <https://doi.org/10.1016/j.atmosenv.2018.08.063>, 2018.
- Wang, C., Li, X., Zhang, T., Tang, A., Cui, M., Liu, X., Ma, X., Zhang, Y., Liu, X., and Zheng, M.: Developing nitrogen isotopic source profiles of atmospheric ammonia for source apportionment of ammonia in urban Beijing, *Front. Environ. Sci.*, 10, <https://doi.org/10.3389/fenvs.2022.903013>, 2022.
- Wang, J., Liu, H., Zhang, Y., Jie, X., Liu, H., Nie, Z., and Zhao, P.: Nitrogen isotope ($\delta^{15}\text{N}$) signatures of ammonia emissions from livestock farming implications for source apportionment of haze pollution, Zenodo [data set], <https://doi.org/10.5281/ZENODO.17639507>, 2025.
- Warner, J. X., Dickerson, R. R., Wei, Z., Strow, L. L., Wang, Y., and Liang, Q.: Increased atmospheric ammonia over the world's major agricultural areas detected from space, *Geophys. Res. Lett.*, 44, 2875–2884, <https://doi.org/10.1002/2016gl072305>, 2017.
- Wong, W. W., Cartwright, I., Poh, S. C., and Cook, P.: Sources and cycling of nitrogen revealed by stable isotopes in a highly populated large temperate coastal embayment, *Sci. Total Environ.*, 806, 150408, <https://doi.org/10.1016/j.scitotenv.2021.150408>, 2022.
- Wu, L., Ren, H., Wang, P., Chen, J., Fang, Y., Hu, W., Ren, L., Deng, J., Song, Y., Li, J., Sun, Y., Wang, Z., Liu, C.-Q., Ying, Q., and Fu, P.: Aerosol ammonium in the urban boundary layer in Beijing: insights from nitrogen isotope ratios and simulations in summer 2015, *Environ. Sci. Technol. Lett.*, 6, 389–395, <https://doi.org/10.1021/acs.estlett.9b00328>, 2019.
- Wu, L., Zhang, Y., Xiao, Y., Zhu, J., Shi, Z., Wang, Y., Xu, H., Hu, W., Deng, J., Tang, M., and Fu, P.: Diversity of ammonia sources in Tianjin: nitrogen isotope analyses and simulations of aerosol ammonium, *Environ. Chem.*, 21, 14482517, <https://doi.org/10.1071/EN24030>, 2024.
- Xi, D., Xiao, Y., Mgelwa, A. S., and Kuang, Y.: Formation pathways and source apportionments of inorganic nitrogen-containing aerosols in urban environment: insights from nitrogen and oxygen isotopic compositions in Guangzhou, China, *Atmos. Environ.*, 309, <https://doi.org/10.1016/j.atmosenv.2023.119888>, 2023.
- Xiang, Y.-K., Dao, X., Gao, M., Lin, Y.-C., Cao, F., Yang, X.-Y., and Zhang, Y.-L.: Nitrogen isotope characteristics and source apportionment of atmospheric ammonium in urban cities during a haze event in northern China plain, *Atmos. Environ.*, 269, 118800–118813, <https://doi.org/10.1016/j.atmosenv.2021.118800>, 2022.
- Xiao, H., Ding, S.-Y., Ji, C.-W., Li, Q.-K., and Li, X.-D.: Combustion related ammonia promotes $\text{PM}_{2.5}$ accumulation in autumn in Tianjin, China, *Atmos. Res.*, 275, <https://doi.org/10.1016/j.atmosres.2022.106225>, 2022.
- Xiao, H., Xiao, H.-W., Xu, Y., Zheng, N.-J., and Xiao, H.-Y.: Combustion-driven inorganic nitrogen in $\text{PM}_{2.5}$ from a city in central China has the potential to enhance the

- nitrogen load of north China, *J. Hazard. Mater.*, 483, <https://doi.org/10.1016/j.jhazmat.2024.136620>, 2025.
- Xiao, H.-W., Wu, J.-F., Luo, L., Liu, C., Xie, Y.-J., and Xiao, H.-Y.: Enhanced biomass burning as a source of aerosol ammonium over cities in central China in autumn, *Environ. Pollut.*, 266, 115278, <https://doi.org/10.1016/j.envpol.2020.115278>, 2020.
- Xie, Y., Xiong, Z., Xing, G., Yan, X., Shi, S., Sun, G., and Zhu, Z.: Source of nitrogen in wet deposition to a rice agroecosystem at tai lake region, *Atmos. Environ.*, 42, 5182–5192, <https://doi.org/10.1016/j.atmosenv.2008.03.008>, 2008.
- Xu, P., Li, G., Zheng, Y., Fung, J. C. H., Chen, A., Zeng, Z., Shen, H., Hu, M., Mao, J., Zheng, Y., Cui, X., Guo, Z., Chen, Y., Feng, L., He, S., Zhang, X., Lau, A. K. H., Tao, S., and Houlton, B. Z.: Fertilizer management for global ammonia emission reduction, *Nature*, 626, 792–798, <https://doi.org/10.1038/s41586-024-07020-z>, 2024.
- Yang, F., Tan, J., Zhao, Q., Du, Z., He, K., Ma, Y., Duan, F., Chen, G., and Zhao, Q.: Characteristics of $\text{PM}_{2.5}$ speciation in representative megacities and across China, *Atmos. Chem. Phys.*, 11, 5207–5219, <https://doi.org/10.5194/acp-11-5207-2011>, 2011.
- Zhang, H., Hong, Z., Wei, L., Thornton, B., Hong, Y., Chen, J., and Zhang, X.: Stable isotopes unravel the sources and transport of $\text{PM}_{2.5}$ in the Yangtze River delta, china, *Atmosphere*, 14, <https://doi.org/10.3390/atmos14071120>, 2023.
- Zhang, L., Altabet, M. A., Wu, T., and Hadas, O.: Sensitive measurement of $\text{NH}_4^+ 15\text{N}/14\text{N}$ ($\delta^{15}\text{NH}_4^+$) at natural abundance levels in fresh and saltwaters, *Anal. Chem.*, 79, 5297–5303, <https://doi.org/10.1021/ac070106d>, 2007.
- Zhou, Y., Zheng, N., Luo, L., Zhao, J., Qu, L., Guan, H., Xiao, H., Zhang, Z., Tian, J., and Xiao, H.: Biomass burning related ammonia emissions promoted a self-amplifying loop in the urban environment in kunming (SW china), *Atmos. Environ.*, 253, <https://doi.org/10.1016/j.atmosenv.2020.118138>, 2021.
- Zou, D., Sun, Q., Liu, J., Xu, C., and Song, S.: Seasonal source analysis of nitrogen and carbon aerosols of $\text{PM}_{2.5}$ in typical cities of Zhejiang, China, *Chemosphere*, 303, <https://doi.org/10.1016/j.chemosphere.2022.135026>, 2022.